



ELSEVIER

# Similarities and differences in the coupling of human $\beta_1$ - and $\beta_2$ -adrenoceptors to $G_{s\alpha}$ splice variants

Katharina Wenzel-Seifert, Hui-Yu Liu<sup>1</sup>, Roland Seifert\*

Department of Pharmacology and Toxicology, The University of Kansas, Malott Hall, Room 5064, 1251 Wescoe Hall Drive, Lawrence, KS 66045, USA

Received 5 September 2001; accepted 2 November 2001

---

## Abstract

The human  $\beta_1$ -adrenoceptor ( $\beta_1$ AR) and  $\beta_2$ -adrenoceptor ( $\beta_2$ AR) couple to  $G_s$ -proteins to activate adenylyl cyclase (AC). There are differences in desensitization between the  $\beta_2$ AR and the originally cloned Gly389- $\beta_1$ AR, but with respect to ternary complex formation, constitutive activity, and AC activation the picture is unclear. To learn more about the similarities and differences between the  $\beta_1$ AR and  $\beta_2$ AR, we analyzed coupling of the Gly389- $\beta_1$ AR to the  $G_{s\alpha}$  splice variants  $G_{s\alpha}L$  and  $G_{s\alpha}S$  using  $\beta_1$ AR- $G_{s\alpha}$  fusion proteins expressed in Sf9 cells and compared the data with previously published data on  $\beta_2$ AR- $G_{s\alpha}$  fusion proteins (Seifert *et al.*, J Biol Chem 1998;273:5109–16). Fusion ensures defined receptor/G-protein stoichiometry and efficient coupling. The agonist (–)-isoproterenol stabilized the ternary complex at  $\beta_1$ AR- $G_{s\alpha}S$ ,  $\beta_1$ AR- $G_{s\alpha}L$ ,  $\beta_2$ AR- $G_{s\alpha}S$ , and  $\beta_2$ AR- $G_{s\alpha}L$  with similar efficiency.  $\beta_1$ AR- $G_{s\alpha}L$  but not  $\beta_1$ AR- $G_{s\alpha}S$  showed the hallmarks of constitutive activity as assessed by increased potencies and efficacies of partial agonists and AC activation by the agonist-free receptor. Similar differences were observed previously for  $\beta_2$ AR- $G_{s\alpha}S$  and  $\beta_2$ AR- $G_{s\alpha}L$ .  $\beta_1$ AR- $G_{s\alpha}S$  and  $\beta_2$ AR- $G_{s\alpha}S$  were similarly efficient at activating AC, but  $\beta_1$ AR- $G_{s\alpha}L$  was ~4-fold more efficient at activating AC than  $\beta_2$ AR- $G_{s\alpha}L$ . Our data show that (i) the  $\beta_1$ AR and  $\beta_2$ AR are similarly efficient at stabilizing the ternary complex with  $G_{s\alpha}$  splice variants, (ii)  $G_{s\alpha}L$  confers constitutive activity to the  $\beta_1$ AR and  $\beta_2$ AR, and (iii) the  $\beta_1$ AR coupled to  $G_{s\alpha}L$  is more efficient at activating AC than the  $\beta_2$ AR coupled to  $G_{s\alpha}L$ . These data help us understand some of the discrepancies regarding similarities and differences between the  $\beta_1$ AR and  $\beta_2$ AR. © 2002 Elsevier Science Inc. All rights reserved.

**Keywords:**  $\beta_1$ -Adrenoceptor;  $\beta_2$ -Adrenoceptor;  $G_{s\alpha}$  splice variants; Constitutive activity; Adenylyl cyclase; Fusion protein

---

\* Corresponding author. Tel.: +1-785-864-3525; fax: +1-785-864-5219.  
E-mail address: rseifert@ku.edu (R. Seifert).

<sup>1</sup> Present address: Neurodegeneration Group, The John P. Robarts Research Institute, London, Ont., Canada.

**Abbreviations:** AC, adenylyl cyclase; ALP, (–)-alprenolol;  $\beta$ AR, non-specified human  $\beta$ -adrenoceptor subtype;  $\beta_1$ AR, human  $\beta_1$ -adrenoceptor (unless explicitly stated otherwise, the Gly389 polymorphism of the  $\beta_1$ AR, i.e. the originally cloned “wild-type”  $\beta_1$ AR with an allele frequency of 0.26 is referred to as the  $\beta_1$ AR);  $\beta_1$ AR- $G_{s\alpha}L$ , fusion protein consisting of the human  $\beta_1$ -adrenoceptor and the long splice variant of  $G_{s\alpha}$ ;  $\beta_1$ AR- $G_{s\alpha}S$ , fusion protein consisting of the human  $\beta_1$ -adrenoceptor and the short splice variant of  $G_{s\alpha}$ ;  $\beta_2$ AR, human  $\beta_2$ -adrenoceptor;  $\beta_2$ AR- $G_{s\alpha}L$ , fusion protein consisting of the human  $\beta_2$ -adrenoceptor and the long splice variant of  $G_{s\alpha}$ ;  $\beta_2$ AR- $G_{s\alpha}S$ , fusion protein consisting of the human  $\beta_2$ -adrenoceptor and the short splice variant of  $G_{s\alpha}$ ; BET, betaxolol; DCI, dichloroisoproterenol; [<sup>3</sup>H]JDHA, [<sup>3</sup>H]dihydroalprenolol; DOB, dobutamine; EPH, (–)-ephedrine;  $G_\alpha$ , non-specified G-protein  $\alpha$ -subunit; GPCR, G-protein-coupled receptor;  $G_{s\alpha}$ , non-specified  $G_s$ -protein, i.e. either  $G_{s\alpha}L$ ,  $G_{s\alpha}S$ , or  $G_{s\alpha}OL$ ;  $G_{s\alpha}L$ , long splice variant of  $G_{s\alpha}$ ;  $G_{s\alpha}S$ , short splice variant of  $G_{s\alpha}$ ; GTP $\gamma$ S, guanosine 5'-O-(3-thiotriphosphate); ICI, ICI 118,551 [erythro-DL-1(7-methylindan-4-yloxy)-3-isopropylaminobutan-2-ol]; ISO, (–)-isoproterenol; LAB, (±)-labetalol; PRA, practolol; PRO, (–)-propranolol; SAL, salbutamol; XAM, xamoterol.

## 1. Introduction

Many hormones and neurotransmitters exert their effects via GPCRs [1–4]. Upon binding of an agonist, GPCRs isomerize from an inactive to an active state, enabling GPCRs to promote GDP dissociation from G-proteins. Not only agonist-occupied but also agonist-free GPCRs can activate G-proteins. Inverse agonists reduce this agonist-independent (constitutive) activity. Agonist-occupied GPCRs form a ternary complex with nucleotide-free G-protein. The ternary complex is characterized by high agonist affinity. GPCRs then promote binding of GTP to  $G_\alpha$ , resulting in ternary complex disruption and dissociation of G-protein into  $G_\alpha$ -GTP and the  $\beta\gamma$ -complex. Both  $G_\alpha$ -GTP and  $\beta\gamma$  regulate the activity of effectors. The GTPase (EC 3.6.1.) of  $G_\alpha$  accomplishes G-protein deactivation by hydrolyzing GTP.  $G_\alpha$ -GDP and  $\beta\gamma$  re-associate, completing the G-protein cycle.

The  $\beta_1$ AR and  $\beta_2$ AR are prototypical GPCRs that couple to  $G_s$ -proteins to activate AC (EC 4.6.1.1) [5]. The human

$\beta_1$ AR exists as two polymorphisms. The originally cloned Gly389- $\beta_1$ AR has an allele frequency of 26% and is less efficient than the Arg389- $\beta_1$ AR (allele frequency 74%) at stabilizing the ternary complex and activating AC [6]. Since the Arg389- $\beta_1$ AR has been identified only recently, most, if not all, published studies aimed at comparing the  $\beta_1$ AR and  $\beta_2$ AR have been conducted with Gly389- $\beta_1$ AR. For this reason, we analyzed Gly389- $\beta_1$ AR in our present study, although future studies will need to directly compare Arg389- $\beta_1$ AR with  $\beta_2$ AR, too.

There is agreement in the literature that the  $\beta_1$ AR is less sensitive to desensitization and internalization than the  $\beta_2$ AR [7–10]. However, with respect to other parameters, the picture is unclear. Freissmuth and coworkers [11] observed a higher percentage of high-affinity binding sites with the  $\beta_2$ AR reconstituted with  $G_s$  than with the  $\beta_1$ AR reconstituted with  $G_s$  using an *Escherichia coli* expression system. In contrast, Green and coworkers [12] found a higher percentage of high-affinity binding sites with the  $\beta_1$ AR than with the  $\beta_2$ AR using CHW cells as the expression system. In the former study, the  $K_h$  values for ISO were similar at the  $\beta_1$ AR and  $\beta_2$ AR, whereas in the latter study the  $K_h$  value for the  $\beta_1$ AR was ~5-fold higher than the  $K_h$  value for the  $\beta_2$ AR. In other studies, it was difficult to discern distinct high-affinity binding sites with the  $\beta_1$ AR [6,13]. When the constitutive activity of the  $\beta_1$ AR and  $\beta_2$ AR is considered, the situation is unclear, too. The  $\beta_1$ AR and  $\beta_2$ AR expressed in HEK293 cells exhibit similarly low extents of constitutive activity [14]. In contrast, the  $\beta_2$ AR expressed in cardiac myocytes from  $\beta_1$ AR/ $\beta_2$ AR double knockout mice exhibits significant constitutive activity, whereas the  $\beta_1$ AR is devoid of any constitutive activity in this expression system [15]. However, when expressed in COS-7 cells, the  $\beta_1$ AR clearly exhibits constitutive activity, although to a lesser extent than the  $\beta_2$ AR [16]. Finally, the data concerning AC activation are controversial. In some studies, the agonist-occupied  $\beta_2$ AR was found to be more efficient at activating AC than the  $\beta_1$ AR [9,17], whereas in other studies the agonist-occupied  $\beta_1$ AR and  $\beta_2$ AR were reported to be similarly efficient at activating AC [7,8,13,14].

The G-protein  $G_s$  exists as two splice variants,  $G_{s_2}L$  and  $G_{s_2}S$ , respectively.  $G_{s_2}L$  possesses a lower GDP affinity than  $G_{s_2}S$  [18,19]. As a result of these biochemical differences between  $G_{s_2}$  splice variants, the agonist-free  $\beta_2$ AR and the  $\beta_2$ AR bound to partial agonists are more efficient at promoting GDP/GTP exchange at  $G_{s_2}L$  than at  $G_{s_2}S$ , i.e.  $G_{s_2}L$  confers the hallmarks of constitutive activity to the  $\beta_2$ AR [19,20]. In addition, the maximum AC activity induced by the  $G_{s_2}L$ -coupled  $\beta_2$ AR is lower than the AC activity induced by the  $G_{s_2}S$ -coupled  $\beta_2$ AR.

Based on these data and the fact that the expression of  $G_{s_2}S$  and  $G_{s_2}L$  varies substantially in different tissues [21], we asked the question whether the analysis of  $\beta_1$ AR-coupling to  $G_{s_2}$  splice variants would help us to understand some of the discrepancies in the literature regarding

differences/similarities between the  $\beta_1$ AR and  $\beta_2$ AR. To address this question, we studied  $\beta_1$ AR- $G_{s_2}$  fusion proteins expressed in Sf9 insect cells and compared their properties with the properties of the previously published  $\beta_2$ AR- $G_{s_2}$  fusion proteins [19,20,22]. In GPCR- $G_\alpha$  fusion proteins, the GPCR C-terminus is linked to the  $G_\alpha$  N-terminus [23–25]. The fusion guarantees a defined 1:1 stoichiometry of the signaling partners, ensures close proximity of the partners, promotes efficient coupling, and allows for the analysis of the coupling of a given GPCR to various G-proteins under defined experimental conditions [19,22]. The expression level of fusion proteins and, thereby, the expression of a specific  $G_\alpha$ , can be precisely determined by GPCR antagonist saturation binding. This information can be used to determine the steady-state GTP turnover of the fusion protein [24,25], the functional integrity of fusion proteins by assessing ligand-regulated GTP $\gamma$ S saturation binding [22,26,27], and the specific efficacies of a given GPCR- $G_{s_2}$  fusion protein at activating AC [27]. Additionally, ternary complex formation, GTP turnover, as well as the efficacies and potencies of partial agonists and inverse agonists in the GTPase and GTP $\gamma$ S binding assays are independent of the expression level of GPCR- $G_\alpha$  fusion proteins [19,22,27,28]. These properties together with the low background signaling of exogenously expressed GPCRs to endogenous insect  $G_s$ -like G-proteins and the very stable AC activity in Sf9 cells render these cells a very sensitive system for the analysis of  $\beta$ ARs [19,28].

## 2. Materials and methods

### 2.1. Materials

The cDNA for the human  $\beta_1$ AR (Gly389 polymorphism) in pUC18 was provided by Dr. M. Bouvier (Department of Biochemistry, University of Montreal). [ $^{35}$ S]GTP $\gamma$ S (1100 Ci/mmol), [ $\gamma$ - $^{32}$ P]GTP (6000 Ci/mmol), and [ $\alpha$ - $^{32}$ P]ATP (3000 Ci/mmol) were from Perkin Elmer. [ $^3$ H]DHA (85–90 Ci/mmol) was from Amersham Pharmacia Biotech. Unlabeled GTP, GTP $\gamma$ S, GDP, and ATP [high quality, catalogue No. 519 979; <0.01% (w/w) GTP contamination as assessed by HPLC analysis] were obtained from Roche Diagnostics. ICI 118,551 (ICI) was from RBI. The M1 monoclonal antibody (detecting the FLAG epitope), ISO, SAL, EPH, DOB, and ALP were from the Sigma Chemical Co. DCI was from the Aldrich Chemical Co. BET, PRA, and XAM were purchased from Tocris Cookson. All restriction enzymes, DNA polymerase I, and T4 DNA ligase were from New England Biolabs. Glass fiber filters (GF/C) were from Schleicher & Schuell.

### 2.2. Construction of the $\beta_1$ AR- $G_{s_2}$ fusion proteins

In the fusion proteins generated in our laboratory, the N-terminus of GPCRs is routinely tagged with the FLAG

epitope, which is recognized by the anti-FLAG Ig (M1 antibody) [28]. The  $G_{\alpha}$  N-terminus is linked to the C-terminus of the GPCRs via a hexahistidine tag. Fusion of the open reading frames of the  $\beta_1$ AR with  $G_{s_2}S$  and  $G_{s_2}L$ , respectively, was achieved by sequential overlap-extension PCRs using *Pfu* polymerase (Stratagene). pUC- $\beta_1$ AR was digested with *Nco*I and *Xba*I, and the *Nco*I/*Xba*I fragment encoding the  $\beta_1$ AR was cloned into pGEM-3Z-FLAG-formyl peptide receptor digested with *Nco*I and *Xba*I to generate pGEM-3Z-FLAG- $\beta_1$ AR. In PCR 1A, the DNA sequence of the C-terminus of  $\beta_1$ AR was amplified with pGEM-3Z-FLAG- $\beta_1$ AR as template by using a sense primer 5' of the *Xho*I site in the C-terminus (sense *Xho*I primer) and an antisense primer encoding the hexahistidine tag. In PCR 1B, the cDNA of  $G_{s_2}L$  was amplified with pGEM-3Z-FLAG- $\beta_2$ AR- $G_{s_2}L$  as template by using a sense primer encoding the hexahistidine tag and an antisense primer encoding the last 5 amino acids of the C-terminus of the  $G_{s_2}$  followed by the stop codon and an extra *Xba*I site for cloning purposes in the 3'-end extension (antisense *Xba*I primer). In PCR 1C, the cDNA of  $G_{s_2}S$  was amplified with pGEM-3Z-FLAG- $\beta_2$ AR- $G_{s_2}S$  as template by using a sense primer encoding the hexahistidine tag and the antisense *Xba*I primer. In PCR 2A, the cDNA fragments from PCRs 1A and 1B were annealed and amplified using the sense *Xho*I primer and the antisense *Xba*I primer. In this way, a fragment encoding the C-terminus of the  $\beta_1$ AR, a hexahistidine tag, and  $G_{s_2}L$  followed by an *Xba*I site was obtained. In PCR 2B, the cDNA fragments from PCRs 1A and 1C were annealed and amplified using the sense *Xho*I primer and the antisense *Xba*I primer. In this way, a fragment encoding the C-terminus of the  $\beta_1$ AR, a hexahistidine tag, and  $G_{s_2}S$  followed by an *Xba*I site was obtained. The fragments of PCRs 2A and 2B were digested with *Xho*I and *Xba*I and cloned into pGEM-3Z-FLAG- $\beta_1$ AR digested with *Xho*I plus *Xba*I. PCR-generated DNA sequences were confirmed by enzymatic sequencing. For generation of the baculovirus expression vector pVL1392, pGEM-3Z- $\beta_1$ AR- $G_{s_2}L$  and pGEM-3Z- $\beta_1$ AR- $G_{s_2}S$  were digested with *Sac*I and *Xba*I and subsequently with *Pvu*II to destroy the pGEM-3Z vector, and fusion protein cDNAs were cloned into pVL1392-FLAG-formyl peptide receptor digested with *Sac*I and *Xba*I.

### 2.3. Generation of recombinant baculoviruses, cell culture, and membrane preparation

Sf9 cells were cultured in 250-mL disposable Erlenmeyer flasks at 28° under rotation at 125 rpm in SF 900 II medium (Invitrogen) supplemented with 5% (v/v) fetal bovine serum (BioWhittaker) and 0.1 mg/mL of gentamicin (BioWhittaker). Cells were maintained at a density of 1.0 to  $6.0 \times 10^6$  cells/mL. Recombinant baculoviruses encoding  $\beta_1$ AR- $G_{s_2}$  fusion proteins were generated in Sf9 cells using the BaculoGOLD transfection kit (Phar-mingen) according to the instructions of the manufacturer.

After initial transfection, high-titer virus stocks were generated by two sequential virus amplifications. In the first amplification, cells were seeded at  $2.0 \times 10^6$  cells/mL and infected with a 1:100 dilution of the supernatant fluid from the initial transfection. Cells were cultured for 7 days, resulting in the death of virtually the entire cell population. The supernatant fluid of this infection was harvested and stored under light protection at 4°. In a second amplification, cells were seeded at  $3.0 \times 10^6$  cells/mL and infected with a 1:20 dilution of the supernatant from the initial amplification. Cells were cultured for 48 hr, and the supernatant fluid was harvested. After the 48-hr culture, the majority of cells showed signs of infections (e.g. altered morphology, viral inclusion bodies), but most of the cells were still intact. The supernatant fluid from the second amplification was also stored under light protection at 4° and was the routine virus stock for membrane preparations. For expression of fusion proteins, Sf9 cells were sedimented by centrifugation (5 min at 500 g at 25°) and suspended in fresh medium. Cells were seeded at  $3.0 \times 10^6$  cells/mL and infected with 1:100 or 1:1000 dilutions of high-titer baculovirus stocks encoding  $\beta_1$ AR- $G_{s_2}L$  or  $\beta_1$ AR- $G_{s_2}S$  fusion proteins. Cells were cultured for 48 hr before membrane preparation. Sf9 membranes were prepared as described previously [28], using 1 mM EDTA, 0.2 mM phenylmethylsulfonyl fluoride, 10 µg/mL of benzamidine, and 10 µg/mL of leupeptin as protease inhibitors. Membranes were suspended in binding buffer (12.5 mM MgCl<sub>2</sub>, 1 mM EDTA, and 75 mM Tris/HCl, pH 7.4), and were stored at -80° for periods of up to 1 year (longer periods of time were not analyzed in this study) without loss of functional activity in the various assays employed.

### 2.4. [<sup>3</sup>H]DHA binding assay

Membranes were thawed, sedimented by a 15-min centrifugation at 4° and 15,000 g to remove residual endogenous guanine nucleotides as far as possible, and resuspended in binding buffer. Expression levels of fusion proteins were determined by incubating Sf9 membranes (25–30 µg protein/tube) in the presence of [<sup>3</sup>H]DHA at concentrations from 0.1 to 10 nM. The total volume of the binding reaction was 500 µL. Incubations were performed for 90 min at 25° on a shaker set at 250 rpm. Non-specific [<sup>3</sup>H]DHA binding was determined in the presence of [<sup>3</sup>H]DHA at various concentrations plus 10 µM (±)-alprenolol. Non-specific [<sup>3</sup>H]DHA binding amounted to less than 10–15% of total [<sup>3</sup>H]DHA binding even with the highest radioligand concentration (10 nM [<sup>3</sup>H]DHA). In agonist-competition studies, tubes contained Sf9 membranes expressing fusion proteins at 3.6–7.5 pmol/mg (25–30 µg protein/tube), 1 nM [<sup>3</sup>H]DHA, and agonists at increasing concentrations. Reaction mixtures additionally contained solvent (control) or GTPγS (10 µM). Bound [<sup>3</sup>H]DHA was separated from free [<sup>3</sup>H]DHA by filtration through GF/C filters using a 48-well harvester (model

M-48R, Brandel), followed by three washes with 2 mL of binding buffer (4°). Filter-bound radioactivity was determined by liquid scintillation counting using Cytoscint fluid from ICN. The experimental conditions chosen ensured that not more than 10% of the total amount of [<sup>3</sup>H]DHA added to binding tubes was bound to filters.

### 2.5. [<sup>35</sup>S]GTP $\gamma$ S binding assay

Membranes were thawed, sedimented by a 15-min centrifugation at 4° and 15,000 g to remove residual endogenous guanine nucleotides as far as possible, and resuspended in binding buffer. For GTP $\gamma$ S saturation binding studies, reaction mixtures (500  $\mu$ L total volume) contained Sf9 membranes expressing fusion proteins at 3.6–7.5 pmol/mg (15–30  $\mu$ g protein/tube) in binding buffer supplemented with 0.05% (w/v) BSA, 1  $\mu$ M GDP, and 0.2–1.0 nM [<sup>35</sup>S]GTP $\gamma$ S plus unlabeled GTP $\gamma$ S at increasing concentrations to give the final ligand concentrations of up to 10 nM. Reaction mixtures additionally contained distilled water (basal) or ISO (10  $\mu$ M). Incubations were performed at 25° for 60 min on a shaker set at 250 rpm. For the analysis of ligand potencies and efficacies, reaction mixtures (500  $\mu$ L total volume) contained Sf9 membranes expressing fusion proteins at 3.6–7.5 pmol/mg (15  $\mu$ g protein/tube) in binding buffer supplemented with 0.05% (w/v) BSA, 1  $\mu$ M GDP, and 0.4 nM [<sup>35</sup>S]GTP $\gamma$ S. Reaction mixtures additionally contained ligands at various concentrations. Incubations were performed at 25° for 60 min on a shaker set at 250 rpm. Non-specific [<sup>35</sup>S]GTP $\gamma$ S binding was determined in the presence of 10  $\mu$ M GTP $\gamma$ S and amounted to less than 0.1% of total [<sup>35</sup>S]GTP $\gamma$ S binding. Bound [<sup>35</sup>S]GTP $\gamma$ S was separated from free [<sup>35</sup>S]GTP $\gamma$ S by filtration through GF/C filters, followed by three washes with 2 mL of binding buffer (4°). Filter-bound radioactivity was determined by liquid scintillation counting using Cytoscint fluid. The experimental conditions chosen ensured that no more than 10% of the total amount of [<sup>35</sup>S]GTP $\gamma$ S added was bound to filters.

### 2.6. AC activity assay

Membranes were thawed, sedimented by a 15-min centrifugation at 4° and 15,000 g to remove residual endogenous guanine nucleotides as far as possible, and resuspended in binding buffer. Tubes contained Sf9 membranes expressing fusion proteins at 0.8–3.8 pmol/mg (15–30  $\mu$ g protein/tube), 5 mM MgCl<sub>2</sub>, 0.4 mM EDTA, 30 mM Tris/HCl, pH 7.4, and GTP at various concentrations without or with ISO (10  $\mu$ M). Assay tubes containing membranes and additions in a total volume of 30  $\mu$ L were incubated for 3 min at 37° before starting reactions by the addition of 20  $\mu$ L of reaction mixture containing (final) [ $\alpha$ -<sup>32</sup>P]ATP (1.0–1.5  $\mu$ Ci/tube) plus 40  $\mu$ M unlabeled ATP, 0.1 mM cAMP, and a regenerating system consisting of 2.7 mM mono-(cyclohexyl)ammonium phosphoenolpyruvate, 0.125 IU

pyruvate kinase, and 1 IU myokinase. We used only high quality ATP from Roche (catalogue No. 519 979; <0.01% GTP content as assessed by HPLC analysis) to minimize exogenous GTP contamination as far as possible. Reactions were conducted for 20 min at 37° and were terminated by the addition of 20  $\mu$ L of 2.2N HCl. Denatured protein was sedimented by a 3-min centrifugation at 25° and 15,000 g, and reaction supernatants (65  $\mu$ L) were applied onto disposable columns filled with 1.3 g of neutral alumina (Sigma A-1522, super I, WN-6). [<sup>32</sup>P]cAMP was separated from [ $\alpha$ -<sup>32</sup>P]ATP by elution of [<sup>32</sup>P]cAMP with 4 mL of 0.1 M ammonium acetate, pH 7.0. Recovery of [<sup>32</sup>P]cAMP was ~80%. Blank values were routinely ~0.01% of the total amount of [ $\alpha$ -<sup>32</sup>P]ATP added. [<sup>32</sup>P]cAMP was determined by liquid scintillation counting using ScintiSafe Econo2 scintillation fluid from Fisher. The experimental conditions chosen ensured that not more than 1–3% of the total amount of [ $\alpha$ -<sup>32</sup>P]ATP added was converted to [<sup>32</sup>P]cAMP.

### 2.7. Steady-state GPase activity assay

Membranes were thawed, sedimented by a 15-min centrifugation at 4° and 15,000 g to remove residual endogenous guanine nucleotides as far as possible, and resuspended in 10 mM Tris/HCl, pH 7.4. Assay tubes contained Sf9 membranes expressing fusion proteins at 3.6–7.5 pmol/mg (10  $\mu$ g protein/tube), 1.0 mM MgCl<sub>2</sub>, 0.1 mM EDTA, 0.1 mM ATP, 1 mM adenylyl imidodiphosphate, 5 mM creatine phosphate, 40  $\mu$ g of creatine kinase, and 0.2% (w/v) bovine serum albumin in 50 mM Tris/HCl, pH 7.4. Tubes additionally contained unlabeled GTP at concentrations between 30 nM and 1  $\mu$ M without or with ISO (10  $\mu$ M). Reaction mixtures (80  $\mu$ L) were incubated for 3 min at 25° before the addition of 20  $\mu$ L of [ $\gamma$ -<sup>32</sup>P]GTP (0.2–0.5  $\mu$ Ci/tube). Reactions were conducted for 20 min at 25°, and were terminated by the addition of 900  $\mu$ L of a suspension consisting of 5% (w/v) activated charcoal and 50 mM NaH<sub>2</sub>PO<sub>4</sub>, pH 2.0. Charcoal absorbs nucleotides but not P<sub>i</sub>. Charcoal-quenched reaction mixtures were centrifuged for 15 min at room temperature at 15,000 g. Seven hundred microliters of the supernatant fluid of reaction mixtures was removed carefully to avoid any aspiration of charcoal, and <sup>32</sup>P<sub>i</sub> was determined by liquid scintillation counting using ScintiSafe Econo2 scintillation fluid. The experimental conditions chosen ensured that not more than 10% of the total amount of [ $\gamma$ -<sup>32</sup>P]GTP added was converted to <sup>32</sup>P<sub>i</sub>.

### 2.8. SDS-PAGE and immunoblot analysis

Membrane proteins were separated on SDS gels containing 10% (w/v) acrylamide. Proteins were then transferred onto Immobilon-P transfer membranes (Millipore) according to the instructions of the manufacturer. Membranes were reacted with anti-FLAG Ig or anti-G<sub>s $\alpha$</sub>  Ig (1:1000

each). Immunoreactive bands were visualized by sheep anti-mouse IgG (anti-FLAG Ig, 1:1000) and donkey anti-rabbit IgG (anti-G<sub>s<sub>x</sub></sub> Ig, 1:1000), respectively, coupled to peroxidase, using *o*-dianisidine and H<sub>2</sub>O<sub>2</sub> as substrates.

### 2.9. Miscellaneous

Protein concentrations were determined using the Bio-Rad DC protein assay kit (Bio-Rad). Data shown in Figs. 2, 3B, and 4 were analyzed by non-linear regression using the Prism III program (GraphPad, Prism). Statistical comparisons were performed using the *t*-test.

## 3. Results and discussion

### 3.1. Analysis of the expression of β<sub>1</sub>AR-G<sub>s<sub>x</sub>L</sub> and β<sub>1</sub>AR-G<sub>s<sub>x</sub>S</sub> in Sf9 membranes by antagonist saturation binding, immunoblotting, and GTPγS saturation binding

Membranes from Sf9 cells infected with high-titer baculovirus stocks encoding β<sub>1</sub>AR-G<sub>s<sub>x</sub>L</sub> and β<sub>1</sub>AR-G<sub>s<sub>x</sub>S</sub> were prepared, and the expression levels of constructs were determined by [<sup>3</sup>H]DHA saturation binding. With a 1:100 dilution of virus stocks, the *B*<sub>max</sub> value (expression levels) of β<sub>1</sub>AR-G<sub>s<sub>x</sub></sub> fusion proteins was 4.5 ± 1.7 pmol/mg (mean ± SD, N = 6). With a 1:1000 dilution of virus stocks, the expression level of β<sub>1</sub>AR-G<sub>s<sub>x</sub></sub> fusion proteins was 1.1 ± 0.4 pmol/mg (mean ± SD, N = 4). β<sub>1</sub>AR-G<sub>s<sub>x</sub>L</sub> bound [<sup>3</sup>H]DHA with a *K<sub>d</sub>* value of 1.6 ± 0.4 nM (mean ± SD, N = 5), and β<sub>1</sub>AR-G<sub>s<sub>x</sub>S</sub> bound [<sup>3</sup>H]DHA with a *K<sub>d</sub>* value of

1.9 ± 0.3 nM (mean ± SD, N = 5). These data show that the expression levels achieved for β<sub>1</sub>AR-G<sub>s<sub>x</sub></sub> are comparable with the expression levels of β<sub>2</sub>AR-G<sub>s<sub>x</sub></sub> fusion proteins [19,27,28] and that the antagonist binding properties of β<sub>1</sub>AR-G<sub>s<sub>x</sub>L</sub> and β<sub>1</sub>AR-G<sub>s<sub>x</sub>S</sub> are similar. Our data also show that by lowering the virus titer by 10-fold, the expression of β<sub>1</sub>AR-G<sub>s<sub>x</sub></sub> fusion proteins was reduced by ~4-fold, which was important for the conduction of AC studies (see below). The maximum expression levels achieved for β<sub>2</sub>AR-G<sub>s<sub>x</sub>L</sub> were substantially higher (~20 pmol/mg) than the expression levels of β<sub>2</sub>AR-G<sub>s<sub>x</sub>S</sub> (~6 pmol/mg), but we did not observe such a difference in the maximum expression level for β<sub>1</sub>AR-G<sub>s<sub>x</sub></sub> fusion proteins.

Sf9 membranes were prepared and analyzed by SDS-PAGE and immunoblotting with the anti-FLAG Ig and the anti-G<sub>s<sub>x</sub></sub> Ig (C-terminal). G<sub>s<sub>x</sub>L</sub> and G<sub>s<sub>x</sub>S</sub> possess molecular masses of 52 and 45 kDa, respectively [18]. The β<sub>1</sub>AR possesses a predicted molecular mass of ~51 kDa [29]. β<sub>1</sub>AR-G<sub>s<sub>x</sub>L</sub> and β<sub>1</sub>AR-G<sub>s<sub>x</sub>S</sub> exhibited apparent molecular masses of ~109–111 and 102–104 kDa, respectively, when probed with the anti-FLAG Ig (Fig. 1A) and anti-G<sub>s<sub>x</sub></sub> Ig (Fig. 1B). The fact that the observed molecular masses of β<sub>1</sub>AR-G<sub>s<sub>x</sub></sub> fusion proteins were slightly higher than the sum of the predicted masses of the β<sub>1</sub>AR and G<sub>s<sub>x</sub></sub> is presumably due to covalent modifications of the β<sub>1</sub>AR. Specifically, the β<sub>1</sub>AR possesses one consensus site for *N*-glycosylation [29], and *N*-glycosylation tends to increase the apparent molecular masses of GPCR-G<sub>α</sub> fusion proteins in SDS-PAGE [27]. We did not observe immunoreactive bands below the β<sub>1</sub>AR-G<sub>s<sub>x</sub></sub> fusion proteins with either of the two antibodies. These findings indicate that the conditions

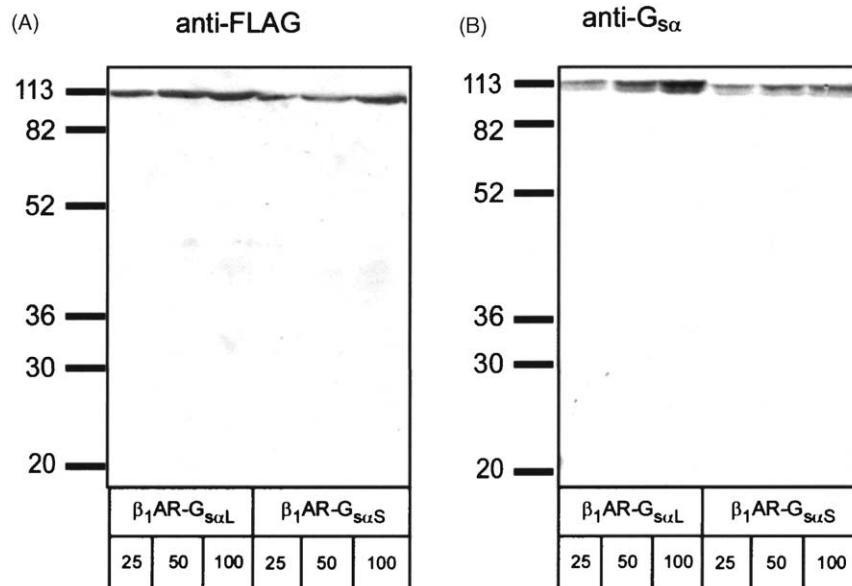


Fig. 1. Analysis of the expression of β<sub>1</sub>AR-G<sub>s<sub>x</sub>L</sub> and β<sub>1</sub>AR-G<sub>s<sub>x</sub>S</sub> in Sf9 membranes. Sf9 cell membranes expressing β<sub>1</sub>AR-G<sub>s<sub>x</sub>L</sub> (4.2 pmol/mg) and β<sub>1</sub>AR-G<sub>s<sub>x</sub>S</sub> (3.0 pmol/mg) were prepared and separated on SDS gels containing 10% (w/v) acrylamide as described in Section 2. Proteins were transferred onto Immobilon-P transfer membranes and probed with anti-FLAG Ig (A) or anti-G<sub>s<sub>x</sub></sub> Ig (B). Shown are the horseradish peroxidase-reacted Immobilon-P transfer membranes. Numbers below fusion proteins indicate the amount of protein (in μg) applied to each lane. Numbers on the left indicate molecular masses of marker proteins.

chosen for cell culture and membrane preparation (see Section 2) efficiently prevented the occurrence of degradation products.

Fusion proteins exhibit a 1:1 GPCR/G<sub>α</sub> stoichiometry [23–25]. Thus, 1 mol of GPCR-G<sub>α</sub> can maximally bind 1 mol of GTPγS provided that both the GPCR and G<sub>α</sub> moieties are functionally intact and that interaction of the GPCRs with the endogenous G-proteins of Sf9 cells is minimal. Inefficient coupling of the β<sub>2</sub>AR to the endogenous G-proteins of the Sf9 cells was documented earlier [19,22,28]. The ratio of the  $B_{max}$  of ligand-regulated GTPγS binding and the  $B_{max}$  of receptor antagonist binding is referred to as a coupling factor [22,27]. To calculate the coupling factor in membranes expressing β<sub>1</sub>AR-G<sub>s<sub>2</sub>S</sub> and β<sub>1</sub>AR-G<sub>s<sub>2</sub>L</sub>, we divided the  $B_{max}$  of ISO-stimulated [<sup>35</sup>S]GTPγS binding by the  $B_{max}$  of [<sup>3</sup>H]DHA binding of the respective membrane preparation. The coupling factors were 0.88 ± 0.16 (mean ± SD, N = 3) for β<sub>1</sub>AR-G<sub>s<sub>2</sub>L</sub> and 0.91 ± 0.19 (mean ± SD, N = 3) for β<sub>1</sub>AR-G<sub>s<sub>2</sub>S</sub>. The  $K_d$  values of ISO-stimulated [<sup>35</sup>S]GTPγS binding were 0.45 ± 0.08 nM (mean ± SD, N = 3) for β<sub>1</sub>AR-G<sub>s<sub>2</sub>L</sub> and 0.81 ± 0.43 nM (mean ± SD, N = 3) for β<sub>1</sub>AR-G<sub>s<sub>2</sub>S</sub>. These data indicate that the majority, if not all of the expressed β<sub>1</sub>AR-G<sub>s<sub>2</sub></sub> fusion protein molecules were functionally intact. Similar coupling factors as for β<sub>1</sub>AR-G<sub>s<sub>2</sub></sub> fusion proteins were obtained for β<sub>2</sub>AR-G<sub>s<sub>2</sub></sub> fusion proteins [22,27]. Additionally, the  $K_d$  values of agonist-stimulated [<sup>35</sup>S]GTPγS binding at β<sub>1</sub>AR-G<sub>s<sub>2</sub></sub> and β<sub>2</sub>AR-G<sub>s<sub>2</sub></sub> fusion proteins are very similar [22,27], indicating that fusion of G<sub>s<sub>2</sub></sub> to different βARs does not change GTPγS affinity of G<sub>s<sub>2</sub></sub>.

### 3.2. Analysis of the agonist binding properties of β<sub>1</sub>AR-G<sub>s<sub>2</sub></sub> and β<sub>2</sub>AR-G<sub>s<sub>2</sub></sub> expressed in Sf9 membranes

Ternary complex formation in β<sub>2</sub>AR-G<sub>s<sub>2</sub></sub> fusion proteins is independent of the fusion protein expression level [19,27,28]. Nonetheless, for the most accurate comparison of data for the β<sub>1</sub>AR and β<sub>2</sub>AR, we ensured that the expression levels of β<sub>1</sub>AR-G<sub>s<sub>2</sub></sub> fusion proteins were in a

similar range (3.6–7.5 pmol/mg) as the expression levels of β<sub>2</sub>AR-G<sub>s<sub>2</sub></sub> fusion proteins (3.3–7.5 pmol/mg) [19]. As for β<sub>2</sub>AR-G<sub>s<sub>2</sub></sub> [19,28], ternary complex formation at β<sub>1</sub>AR-G<sub>s<sub>2</sub></sub> was determined indirectly by agonist-competition of [<sup>3</sup>H]DHA binding. We analyzed the agonists ISO, SAL, and DOB. Fig. 2 shows the agonist-competition isotherms, and Table 1 summarizes the non-linear regression analysis of the binding data. For all three agonists, we obtained biphasic competition curves at β<sub>1</sub>AR-G<sub>s<sub>2</sub>L</sub> and β<sub>1</sub>AR-G<sub>s<sub>2</sub>S</sub> in the absence of GTPγS. These data show that ISO, SAL, and DOB stabilized the ternary complex with a fraction of the available β<sub>1</sub>AR-G<sub>s<sub>2</sub></sub> molecules. The question as to why agonists do not stabilize the ternary complex in all fusion protein molecules present has been discussed earlier [30,31]. In accordance with previous results obtained for the β<sub>2</sub>AR [19] and turkey βAR [32], GTPγS shifted the agonist-competition curves to the right and rendered them monophasic, indicative of ternary complex disruption. The efficiency of a given agonist at stabilizing the ternary complex was similar at β<sub>1</sub>AR-G<sub>s<sub>2</sub>S</sub> and β<sub>1</sub>AR-G<sub>s<sub>2</sub>L</sub> as expressed by the percentage of high-affinity binding sites. Similar data were obtained for β<sub>2</sub>AR-G<sub>s<sub>2</sub>S</sub> and β<sub>2</sub>AR-G<sub>s<sub>2</sub>L</sub> [19]. The  $K_h$  values for ISO at β<sub>1</sub>AR-G<sub>s<sub>2</sub></sub> fusion proteins were similar to the corresponding  $K_h$  values for ISO at β<sub>2</sub>AR-G<sub>s<sub>2</sub></sub> fusion proteins (Table 1) [19]. Moreover, the percentages of high-affinity binding sites at β<sub>1</sub>AR-G<sub>s<sub>2</sub></sub> and β<sub>2</sub>AR-G<sub>s<sub>2</sub></sub> fusion proteins with ISO were very similar (~40–50%). Taken together, the ability of a given βAR at stabilizing the ternary complex with a specific ligand is independent of the particular G<sub>s<sub>2</sub></sub> splice variant to which the GPCR is fused. In addition, ISO is similarly efficient at stabilizing the ternary complex at the two β<sub>1</sub>AR-G<sub>s<sub>2</sub></sub> and the two β<sub>2</sub>AR-G<sub>s<sub>2</sub></sub> fusion proteins. Previous studies yielded inconsistent results regarding the ability of ISO at stabilizing the ternary complex at the β<sub>1</sub>AR and β<sub>2</sub>AR [6,11–13]. An explanation for these differences could be different βAR/G<sub>s</sub> stoichiometries and/or different βAR/G<sub>s</sub> compartmentalizations in the various assay systems. Our data show that annihilation of differences in stoichiometry and/or compartments by the use of the GPCR-G<sub>α</sub> fusion protein

Table 1

Analysis of the agonist binding properties of β<sub>1</sub>AR-G<sub>s<sub>2</sub>L</sub> and β<sub>1</sub>AR-G<sub>s<sub>2</sub>S</sub> expressed in Sf9 membranes

Agonist	$K_h$ (nM)	$K_l$ (nM)	%R <sub>h</sub>	$K_{IGTP\gamma S}$ (nM)
β <sub>1</sub> AR-G <sub>s<sub>2</sub>L</sub>				
ISO	2.0 (0.6–6.8)	90 (40–200)	42.2 (23.4–61.0)	46 (30–70)
SAL	19 (8.0–35)	3900 (2500–6200)	13.6 (4.0–23.5)	4900 (3900–6100)
DOB	9.5 (3.5–25)	1700 (1200–2400)	25.1 (18.5–31.6)	1400 (1200–1800)
β <sub>1</sub> AR-G <sub>s<sub>2</sub>S</sub>				
ISO	0.9 (0.7–1.1)	90 (78–100)	39.6 (66.9–42.2)	54 (42–68)
SAL	2.9 (0.7–13)	4700 (3700–6100)	16.5 (11.9–21.1)	5500 (4700–6400)
DOB	8.6 (2.4–28)	1800 (1200–2700)	23.2 (15.6–30.6)	3600 (2400–5300)

Agonist-competition binding in Sf9 membranes expressing β<sub>1</sub>AR-G<sub>s<sub>2</sub></sub> was performed as described in Section 2. The data shown in Fig. 2 were analyzed by non-linear regression for the best fit to monophasic or biphasic competition curves. Data shown are the means of 3–4 experiments performed in triplicate. Number in parentheses represent the 95% confidence intervals.  $K_h$  and  $K_l$  designate the dissociation constants for the high- and low-affinity state of the β<sub>1</sub>AR, respectively. %R<sub>h</sub> indicates the percentage of high-affinity binding sites. The dissociation constants obtained in the presence of GTPγS (10 μM) are listed under  $K_{IGTP\gamma S}$ .

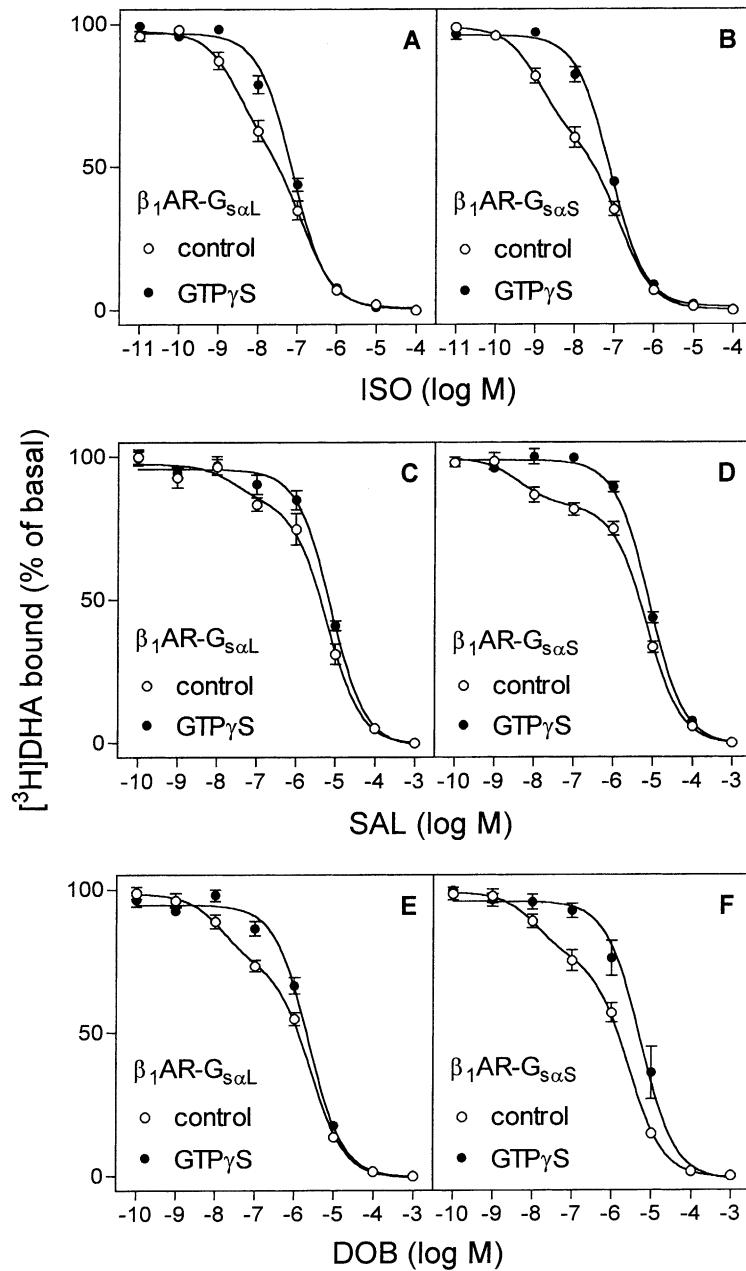


Fig. 2. Competition by ISO, SAL, and DOB of [<sup>3</sup>H]DHA binding in Sf9 membranes expressing  $\beta_1$ AR- $G_{s\alpha}L$  and  $\beta_1$ AR- $G_{s\alpha}S$ : effect of GTP $\gamma$ S. [<sup>3</sup>H]DHA binding was performed as described in Section 2. Reaction mixtures contained Sf9 membranes expressing  $\beta_1$ AR- $G_{s\alpha}L$  (A, C, and E) or  $\beta_1$ AR- $G_{s\alpha}S$  (B, D, and F), 1 nM [<sup>3</sup>H]DHA, and agonists at increasing concentrations. Reaction mixtures additionally contained distilled water (control, ○) or 10  $\mu$ M GTP $\gamma$ S (●). Data points shown are the means  $\pm$  SD of 3–4 experiments. Data were analyzed by non-linear regression for best fit to monophasic or biphasic competition curves. The results of this analysis are summarized in Table 1. Typical absolute [<sup>3</sup>H]DHA binding values in the absence of competitor were ~2000–6000 cpm, depending upon the amount of protein added and the expression level of fusion proteins.

technique abolishes potential differences in the ability of the  $\beta_1$ AR and  $\beta_2$ AR at stabilizing the ternary complex with ISO.

### 3.3. Ligand potencies and efficacies at $\beta_1$ AR- $G_{s\alpha}L$ and $\beta_1$ AR- $G_{s\alpha}S$ expressed in Sf9 membranes

The steady-state GTPase assay and GTP $\gamma$ S binding assay are equally feasible for determining ligand potencies and efficacies at GPCR- $G_\alpha$  fusion proteins [19,22,26,33]. In the

present study, we determined ligand efficacies in the GTP $\gamma$ S binding assay. At  $\beta_1$ AR- $G_{s\alpha}L$ , agonists-stimulated GTP $\gamma$ S binding in the order of efficacy ISO ~ SAL ~ DOB > XAM > EPH > DCI > PRA > LAB ~ ALP > PRO (Fig. 3A). ICI and BET acted as weak inverse agonists at  $\beta_1$ AR- $G_{s\alpha}L$ . With the exception of ISO, being a full agonist at both fusion proteins, and ICI, the efficacies of all other ligands were significantly lower at  $\beta_1$ AR- $G_{s\alpha}S$  than at  $\beta_1$ AR- $G_{s\alpha}L$ . The differences in agonist/inverse agonist efficacies at  $\beta_1$ AR- $G_{s\alpha}L$  versus  $\beta_1$ AR- $G_{s\alpha}S$  resulted in a

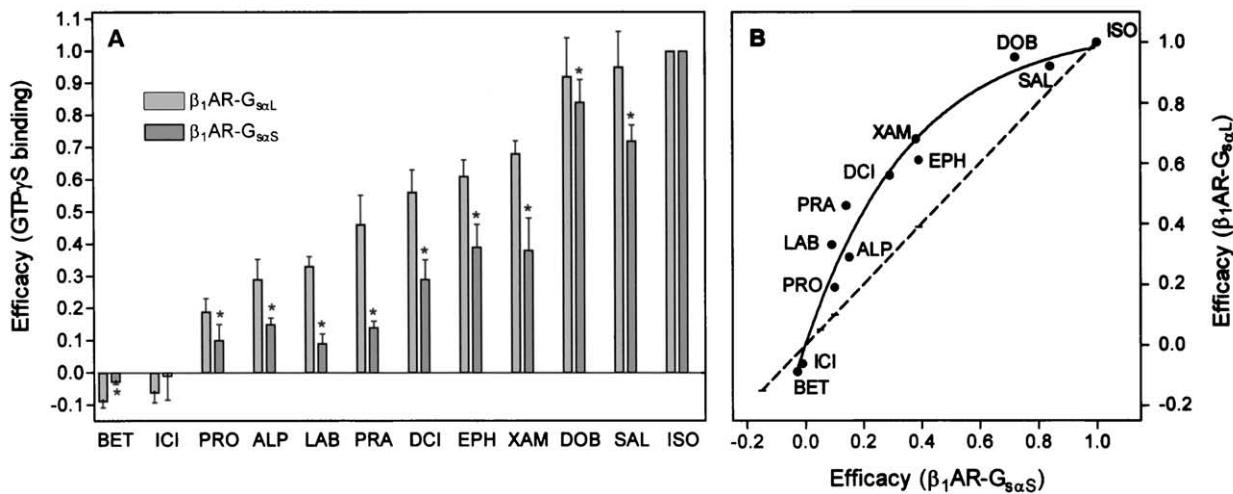


Fig. 3. Efficacies of partial agonists at  $\beta_1$ AR- $G_{s_2}L$  and  $\beta_1$ AR- $G_{s_2}S$  in the GTP $\gamma$ S binding assay. GTP $\gamma$ S binding in Sf9 membranes expressing  $\beta_1$ AR- $G_{s_2}L$  and  $\beta_2$ AR- $G_{s_2}S$  was determined as described in Section 2. Reaction mixtures contained Sf9 membranes expressing fusion proteins, 1  $\mu$ M GDP, 0.4 nM [ $^{35}$ S]GTP $\gamma$ S, and ISO, SAL, DOB, EPH, and DCI at concentrations between 0.1 nM and 100  $\mu$ M as appropriate to obtain saturated concentration/response curves. Efficacies were determined by using the baseline and plateau values of the non-linear regression analysis of concentration/response curves. For determination of the efficacies of XAM, PRA, LAB, ALP, PRO, ICI, and BET, we used ligands at a single fixed concentration (10  $\mu$ M). The effect of ISO at each fusion protein was set at 1.00, and the effects of other ligands were referred to this value. Data shown in panel A represent the means  $\pm$  SD of 4–5 experiments performed in triplicate. The effects of a given ligand at  $\beta_1$ AR- $G_{s_2}L$  versus  $\beta_1$ AR- $G_{s_2}S$  were compared using the *t*-test. Key: (\*)  $P < 0.05$ . In panel B, the efficacies of ligands at  $\beta_1$ AR- $G_{s_2}S$  were plotted against the efficacies of ligands at  $\beta_1$ AR- $G_{s_2}L$ . Data were best fitted to a monophasic saturation hyperbola ( $r^2$ , 0.97). The straight dashed line represents the theoretical curve that would have resulted if the efficacies of ligands at  $\beta_1$ AR- $G_{s_2}L$  and  $\beta_1$ AR- $G_{s_2}S$  had been identical.

hyperbolic relation when the ligand efficacies at  $\beta_1$ AR- $G_{s_2}S$  were plotted against the efficacies at  $\beta_1$ AR- $G_{s_2}L$  (Fig. 3B). Thus, the increase in efficacy of agonists at  $\beta_1$ AR- $G_{s_2}L$  was most pronounced for agonists with intermediate efficacies (LAB → XAM). The differences in agonist efficacies were accompanied by similar changes in agonist potencies, i.e. at  $\beta_1$ AR- $G_{s_2}L$  the potencies of partial agonists and the full agonist ISO were all higher than at  $\beta_1$ AR- $G_{s_2}S$  (Table 2). These data together with the strong stimulatory effect of GTP on basal AC activity in membranes expressing  $\beta_1$ AR- $G_{s_2}L$  (Fig. 4A), reflecting GDP/GTP exchange catalyzed by the agonist-free  $\beta_1$ AR, show that the  $\beta_1$ AR coupled to  $G_{s_2}L$  exhibits the hallmarks of constitutive activity [19,34]. For the  $\beta_2$ AR- $G_{s_2}L/\beta_2$ AR- $G_{s_2}S$  couple, we observed similar

differences in efficacies and potencies for SAL, DOB, EPH, and DCI as for the  $\beta_1$ AR- $G_{s_2}L/\beta_1$ AR- $G_{s_2}S$  couple (Fig. 3) [19]. Additionally, the relative stimulatory effects of GTP on AC activity are similar in membranes expressing  $\beta_1$ AR- $G_{s_2}L$  and  $\beta_2$ AR- $G_{s_2}L$  (Fig. 4A) [20,35]. Collectively, our data indicate that  $G_{s_2}L$  confers similar extents of constitutive activity to the  $\beta_1$ AR and  $\beta_2$ AR.

Our data may help in reconciling some of the divergent results in the literature regarding the constitutive activity of the  $\beta_1$ AR compared with the constitutive activity of the  $\beta_2$ AR [14–16]. Specifically, the  $\beta_1$ AR expressed in cardiac myocytes from  $\beta_1$ AR/ $\beta_2$ AR double knockout mice could be exclusively coupled to  $G_{s_2}S$ , resulting in the absence of constitutive activity [15]. In contrast, in this system, the  $\beta_2$ AR could efficiently couple to  $G_{s_2}L$ , resulting in significant constitutive activity. In transfected HEK293 cells, both the  $\beta_1$ AR and  $\beta_2$ AR may couple more efficiently to  $G_{s_2}S$  than to  $G_{s_2}L$ , resulting in low but measurable constitutive activity of both  $\beta$ ARs [14]. Finally, the  $\beta_1$ AR expressed in COS-7 cells may couple quite efficiently to  $G_{s_2}L$ , resulting in significant constitutive activity of the  $\beta_1$ AR [16]. However, in this system, the  $\beta_2$ AR could couple more efficiently to  $G_{s_2}L$  than the  $\beta_1$ AR, since the  $\beta_2$ AR exhibits higher constitutive activity than the  $\beta_1$ AR. Taken together, our results and the results from other investigators suggest that in different expression systems, the  $\beta_1$ AR and  $\beta_2$ AR have differential access to  $G_{s_2}$  splice variants, resulting in differential activation of  $G_{s_2}S$  and  $G_{s_2}L$  by the two  $\beta$ ARs. In fact, there is precedence for differential activation of  $G_{s_2}$  splice variants by various GPCRs in native systems [36]. Future studies will have

Table 2  
Potencies of full and partial agonists at stimulating GTP $\gamma$ S binding in Sf9 membranes expressing  $\beta_1$ AR- $G_{s_2}L$  and  $\beta_1$ AR- $G_{s_2}S$

Ligand	$\beta_1$ AR- $G_{s_2}L$ (EC <sub>50</sub> , nM)	$\beta_1$ AR- $G_{s_2}S$ (EC <sub>50</sub> , nM)
ISO	2.8 $\pm$ 1.5	10.5 $\pm$ 2.1*
SAL	530 $\pm$ 231	1370 $\pm$ 303*
DOB	133 $\pm$ 62	400 $\pm$ 117*
EPH	1670 $\pm$ 503	4720 $\pm$ 2860*
DCI	13.1 $\pm$ 2.5	39 $\pm$ 15*

Measurement of GTP $\gamma$ S binding in Sf9 membranes expressing  $\beta_1$ AR- $G_{s_2}L$  and  $\beta_1$ AR- $G_{s_2}S$  was performed as described under Section 2. Reaction mixture contained ligands at concentrations between 0.1 nM and 100  $\mu$ M as appropriate to obtain saturated concentration/response curves. Data were best fitted to sigmoidal concentration/response curves. Data shown are the mean  $\pm$  SD of 4–5 experiments performed in triplicate.

\* The EC<sub>50</sub> values of ligands at  $\beta_1$ AR- $G_{s_2}L$  were compared versus the corresponding EC<sub>50</sub> values of ligands at  $\beta_1$ AR- $G_{s_2}S$  with *t*-test;  $P < 0.05$ .

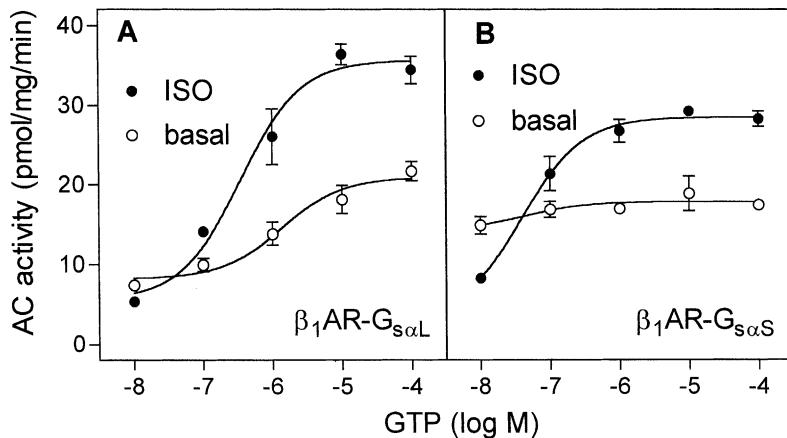


Fig. 4. Regulation of AC activity in Sf9 membranes by  $\beta_1\text{AR-G}_{s_2}\text{L}$  and  $\beta_1\text{AR-G}_{s_2}\text{S}$ . AC activity in Sf9 membranes was determined as described in Section 2. Reaction mixtures contained Sf9 membranes expressing  $\beta_1\text{AR-G}_{s_2}\text{L}$  (0.8 pmol/mg, panel A) or  $\beta_1\text{AR-G}_{s_2}\text{S}$  (1.1 pmol/mg, panel B), GTP at the concentrations indicated on the abscissa ( $10^{-8}$  designates the absence of added GTP) plus solvent (basal, ○) or ISO (10  $\mu\text{M}$ , ●). The commercial ATP preparation used (Roche No. 519 979) contains <0.01% (w/w) GTP. Given an ATP concentration of 40  $\mu\text{M}$ , the maximum GTP concentration in the absence of added GTP was <4 nM. Data were analyzed by non-linear regression and were best fitted to sigmoidal concentration/response curves. Data shown are the means  $\pm$  SD of 3 experiments performed in duplicate.

to determine the expression levels of  $G_{s_2}$  splice variants in various expression systems and the localization of  $G_{s_2}$  splice variants relative to the  $\beta_1\text{AR}$  and  $\beta_2\text{AR}$ . Moreover, differential activation of  $G_{s_2}$  splice variants by the  $\beta_1\text{AR}$  and  $\beta_2\text{AR}$  has to be verified in those systems.

#### 3.4. Regulation of AC activity in Sf9 membranes expressing $\beta_1\text{AR-G}_{s_2}\text{L}$ and $\beta_1\text{AR-G}_{s_2}\text{S}$

For comparing  $\beta_1\text{AR-G}_{s_2}\text{L}$  and  $\beta_1\text{AR-G}_{s_2}\text{S}$  in terms of AC regulation it was important to express fusion proteins at similar levels, ensuring comparable fusion protein/AC ratios and to avoid excessively high expression levels because this leads to a depletion of the available AC molecules [27,28,37]. We performed AC studies at low (0.8–1.3 pmol/mg) and intermediate (3.6–3.8 pmol/mg)  $\beta_1\text{AR-G}_{s_2}$  expression levels. Fig. 4 shows the GTP-dependency of AC activity in membranes expressing  $\beta_1\text{AR-G}_{s_2}\text{L}$  and  $\beta_1\text{AR-G}_{s_2}\text{S}$  at a low level, and Table 3 shows results obtained for membranes expressing  $\beta_1\text{AR-G}_{s_2}$  at different

levels. In membranes expressing  $\beta_1\text{AR-G}_{s_2}\text{L}$ , GTP increased basal AC activity with an  $EC_{50}$  of 1.4  $\mu\text{M}$  (95% confidence interval, 0.64–3.1  $\mu\text{M}$ ) and by  $\sim 250\%$ . The stimulatory effect of GTP on basal AC activity reflects the constitutive activity of the  $\beta_1\text{AR}$  (see above). ISO shifted the concentration/response curve for GTP in membranes expressing  $\beta_1\text{AR-G}_{s_2}\text{L}$   $\sim 4$ -fold to the left ( $EC_{50}$ , 0.35  $\mu\text{M}$ ; 95% confidence interval, 0.19–0.66  $\mu\text{M}$ ) and increased AC activity by  $\sim 100$  and 60% above basal with GTP concentrations of 10 and 100  $\mu\text{M}$ , respectively.

The basal AC activity in membranes expressing  $\beta_1\text{AR-G}_{s_2}\text{S}$  was  $\sim 2$ -fold higher than in membranes expressing  $\beta_1\text{AR-G}_{s_2}\text{L}$ . GTP had a much smaller stimulatory effect on basal AC activity in membranes expressing  $\beta_1\text{AR-G}_{s_2}\text{S}$  than in membranes expressing  $\beta_1\text{AR-G}_{s_2}\text{L}$ , reflecting the low constitutive activity of the  $G_{s_2}\text{-coupled } \beta_1\text{AR}$  (see above). In the presence of GTP, ISO exhibited a significant stimulatory effect on AC activity in membranes expressing  $\beta_1\text{AR-G}_{s_2}\text{S}$  ( $\sim 45\%$ ), but the maximum ISO-stimulated AC activities in membranes expressing  $\beta_1\text{AR-G}_{s_2}\text{S}$  at a low

Table 3  
Regulation of AC activity in Sf9 membranes expressing  $\beta_1\text{AR-G}_{s_2}\text{L}$  and  $\beta_1\text{AR-G}_{s_2}\text{S}$  at low and intermediate levels

Expression level (pmol/mg)	AC activity (pmol/mg/min)				Stimulatory effect of GTP (%)	Stimulatory effect of ISO with GTP (%)
	–GTP, –ISO	–GTP, +ISO	+GTP, –ISO	+GTP, +ISO		
$\beta_1\text{AR-G}_{s_2}\text{L}$						
0.8	6.6 $\pm$ 1.1	5.3 $\pm$ 0.1	23.4 $\pm$ 2.3	37.5 $\pm$ 4.2	254.5	60.3
3.6	9.8 $\pm$ 1.7	9.3 $\pm$ 1.0	37.4 $\pm$ 2.4	45.9 $\pm$ 3.8	281.6	22.7
$\beta_1\text{AR-G}_{s_2}\text{S}$						
1.1	14.0 $\pm$ 1.3	8.6 $\pm$ 2.7	17.6 $\pm$ 0.3	26.8 $\pm$ 2.1	25.7	46.0
3.8	25.3 $\pm$ 1.1	18.9 $\pm$ 0.8	36.0 $\pm$ 2.2	45.5 $\pm$ 4.6	42.2	26.3

Membranes from Sf9 cells expressing  $\beta_1\text{AR-G}_{s_2}$  at various levels as determined by [<sup>3</sup>H]DHA saturation binding were prepared. AC activity in membranes expressing  $\beta_1\text{AR-G}_{s_2}$  was determined as described in Section 2. Reaction mixtures contained no addition (–GTP, –ISO), 10  $\mu\text{M}$  ISO (–GTP, +ISO), 100  $\mu\text{M}$  GTP (+GTP, –ISO), or 100  $\mu\text{M}$  GTP plus 10  $\mu\text{M}$  ISO (+GTP, +ISO). The relative stimulatory effects of GTP (+GTP, –ISO versus –GTP, –ISO) and ISO (+GTP, +ISO versus +GTP, –ISO) were calculated as well. Data shown are the means  $\pm$  SD of three experiments performed in duplicate.

level were lower than the AC activities observed with  $\beta_1$ AR-G<sub>s<sub>2</sub>L</sub> expressed at a similar level.

In membranes expressing  $\beta_1$ AR-G<sub>s<sub>2</sub>S</sub>, ISO exhibited a profound *inhibitory* effect on AC activity in the absence of GTP. This inhibition is explained by the fact that in the absence of GTP, the agonist-occupied  $\beta_1$ AR can only promote GDP dissociation from, but not GTP binding to, G<sub>s<sub>2</sub></sub>. Since G<sub>s<sub>2</sub>-GDP</sub> is more efficient at activating AC than nucleotide-free G<sub>s<sub>2</sub></sub> [19,27], agonist stimulation actually decreases AC activity. The lower GDP affinity of G<sub>s<sub>2</sub>L</sub> relative to G<sub>s<sub>2</sub>S</sub> explains the lower basal AC activity in membranes expressing  $\beta_1$ AR-G<sub>s<sub>2</sub>L</sub> and the lack of inhibitory effect of ISO on basal AC activity in the absence of GTP [18,19]. A very similar pattern of AC regulation in the absence of GTP as for  $\beta_1$ AR-G<sub>s<sub>2</sub></sub> was observed for  $\beta_2$ AR-G<sub>s<sub>2</sub></sub> fusion proteins [19,27].

With  $\beta_1$ AR-G<sub>s<sub>2</sub>L</sub> expressed at  $\sim$ 1 pmol/mg, we obtained ISO-stimulated AC activity of  $\sim$ 35–40 pmol/mg/min. If there had been a linear relation between fusion protein expression level and AC activation, we would have expected to observe ISO-stimulated AC activities of  $\sim$ 125–140 pmol/mg/min in membranes expressing  $\beta_1$ AR-G<sub>s<sub>2</sub>L</sub> at  $\sim$ 3.5 pmol/mg. However, the maximum ISO-stimulated AC activities in membranes expressing  $\beta_1$ AR-G<sub>s<sub>2</sub>L</sub> did not exceed  $\sim$ 45 pmol/mg/min. These data indicate depletion of AC molecules with  $\beta_1$ AR-G<sub>s<sub>2</sub>L</sub> expressed at high levels. With respect to basal AC activities, ISO inhibition of AC in the absence of GTP, and the stimulatory effects of GTP on basal AC activity, similar patterns of AC regulation were observed with  $\beta_1$ AR-G<sub>s<sub>2</sub></sub> expressed at low and intermediate levels. However, because of AC depletion, the relative stimulatory effects of ISO were smaller in membranes expressing fusion proteins at intermediate levels than in membranes expressing  $\beta_1$ AR-G<sub>s<sub>2</sub></sub> at low levels. The depletion of AC molecules with  $\beta_1$ AR-G<sub>s<sub>2</sub>L</sub> at a level of 3.6 pmol/mg was, nonetheless, surprising, given the fact that with  $\beta_2$ AR-G<sub>s<sub>2</sub>L</sub>, AC depletion is only observed with fusion protein expression levels of  $>7.0$  pmol/mg [28]. We also noted that with  $\beta_1$ AR-G<sub>s<sub>2</sub>L</sub> expressed at  $\sim$ 1 pmol/mg, the maximum ISO-stimulated AC activities were almost 2-fold higher than the corresponding AC activities with  $\beta_2$ AR-G<sub>s<sub>2</sub>L</sub> expressed at  $\sim$ 2.5 pmol/mg [35].

To compare the efficacies of  $\beta_1$ AR-G<sub>s<sub>2</sub></sub> and  $\beta_2$ AR-G<sub>s<sub>2</sub></sub> at activating AC in an expression level-independent manner, we divided AC activities by the expression levels of fusion proteins (Table 4). The numbers obtained represent the specific efficacies of a given fusion protein at activating AC [27]. For these calculations, we considered only AC activities obtained with fusion proteins expressed at levels that did not deplete AC molecules.  $\beta_2$ AR-G<sub>s<sub>2</sub>L</sub> exhibited a 2- to 5-fold lower specific efficacy than  $\beta_2$ AR-G<sub>s<sub>2</sub>S</sub> at activating AC, depending on the particular experimental condition considered. The specific efficacy of  $\beta_1$ AR-G<sub>s<sub>2</sub>L</sub> at activating AC in the absence of GTP was 30% lower than that of  $\beta_1$ AR-G<sub>s<sub>2</sub>S</sub>, whereas the specific efficacy of  $\beta_1$ AR-G<sub>s<sub>2</sub>L</sub> in

Table 4

Specific efficacies of  $\beta_1$ AR-G<sub>s<sub>2</sub></sub> and  $\beta_2$ AR-G<sub>s<sub>2</sub></sub> at activating AC in Sf9 membranes

Fusion protein	Specific efficacy at activating AC (min <sup>-1</sup> )		
	-GTP, -ISO	+GTP, -ISO	+GTP, +ISO
$\beta_1$ AR-G <sub>s<sub>2</sub>L</sub>	7.3 $\pm$ 2.8	24.9 $\pm$ 3.1	39.9 $\pm$ 4.5
$\beta_1$ AR-G <sub>s<sub>2</sub>S</sub>	11.7 $\pm$ 0.3	14.8 $\pm$ 2.1	22.4 $\pm$ 0.8
$\beta_2$ AR-G <sub>s<sub>2</sub>L</sub>	2.0 $\pm$ 0.3	6.8 $\pm$ 0.9	9.4 $\pm$ 1.7
$\beta_2$ AR-G <sub>s<sub>2</sub>S</sub>	9.6 $\pm$ 1.4	14.3 $\pm$ 2.1	22.5 $\pm$ 2.3

AC activity in Sf9 membranes expressing  $\beta_1$ AR-G<sub>s<sub>2</sub></sub> (0.81–1.3 pmol/mg) or  $\beta_2$ AR-G<sub>s<sub>2</sub></sub> (2.0–3.0 pmol/mg) was determined as described in Section 2. Reaction mixtures contained no addition (-GTP, -ISO), 100  $\mu$ M GTP (+GTP, -ISO), or 100  $\mu$ M GTP plus 10  $\mu$ M ISO (+GTP, +ISO). AC activities (in pmol/mg/min) were divided by the respective expression levels of fusion protein (in pmol/mg) to obtain the specific efficacies of fusion proteins at activating AC. The raw data for  $\beta_2$ AR-G<sub>s<sub>2</sub>L</sub> and  $\beta_2$ AR-G<sub>s<sub>2</sub>S</sub> were taken from [19,20,27]. Data shown are the means  $\pm$  SD of 3–5 experiments with different membrane preparations performed in duplicate.

the presence of GTP and GTP plus ISO was  $\sim$ 70–80% higher than the specific efficacy of  $\beta_1$ AR-G<sub>s<sub>2</sub>S</sub>. The specific efficacies of  $\beta_1$ AR-G<sub>s<sub>2</sub>S</sub> and  $\beta_2$ AR-G<sub>s<sub>2</sub>S</sub> at activating AC were very similar, whereas the specific efficacy of  $\beta_1$ AR-G<sub>s<sub>2</sub>L</sub> was  $\sim$ 4-fold higher than the efficacy of  $\beta_2$ AR-G<sub>s<sub>2</sub>L</sub> under all experimental conditions analyzed.

Several possibilities have to be discussed to explain the differences in specific efficacies of fusion proteins at activating AC. First, differences in G-protein deactivation have to be considered. Specifically, G<sub>s<sub>2</sub>L</sub> coupled to the  $\beta_1$ AR could be  $\sim$ 4 times more frequent in the active GTP-bound state than G<sub>s<sub>2</sub>L</sub> coupled to the  $\beta_2$ AR. If this model were correct, we would expect considerably higher ISO-stimulated GTPase activities with  $\beta_2$ AR-G<sub>s<sub>2</sub>L</sub> than with  $\beta_1$ AR-G<sub>s<sub>2</sub>L</sub>. In fact, an inverse relation between maximum agonist-stimulated steady-state GTP hydrolysis and effector system activation was observed for various systems [27,38]. The V<sub>max</sub> of the ISO-stimulated GTP hydrolysis of  $\beta_1$ AR-G<sub>s<sub>2</sub>L</sub> was  $2.90 \pm 0.16$  min<sup>-1</sup> (mean  $\pm$  SD, N = 3) and was actually  $\sim$ 2-fold higher than the V<sub>max</sub> of ISO-stimulated GTP hydrolysis of  $\beta_2$ AR-G<sub>s<sub>2</sub>L</sub> ( $1.37 \pm 0.11$  min<sup>-1</sup>) [35]. ISO-stimulated GTP hydrolysis in  $\beta_1$ AR-G<sub>s<sub>2</sub>S</sub> with a V<sub>max</sub> of  $2.66 \pm 0.10$  min<sup>-1</sup> (mean  $\pm$  SD, N = 3). These data argue against the hypothesis that differences in G-protein deactivation account for the differences in specific efficacies of  $\beta_1$ AR-G<sub>s<sub>2</sub></sub> and  $\beta_2$ AR-G<sub>s<sub>2</sub></sub> at activating AC. Second, one has to consider that  $\beta$ ARs and G<sub>s<sub>2</sub></sub> are in contact with each other during the entire G-protein cycle and that GPCRs confer specific conformations to a given G-protein. Specifically, the  $\beta_1$ AR may confer to G<sub>s<sub>2</sub>L</sub> a more active conformation with respect to AC activation than the  $\beta_2$ AR. Additionally, the G<sub>s<sub>2</sub>L</sub> conformation stabilized by the  $\beta_1$ AR may be more active than the corresponding G<sub>s<sub>2</sub>S</sub> conformation, whereas the opposite may be true for the  $\beta_2$ AR. There is already evidence for continuous interaction of GPCRs with G-proteins and effector during the entire G-protein cycle [22,35,39–41]. Third, one must consider that the individual

$\beta$ AR-G<sub>s<sub>z</sub></sub> fusion proteins and the endogenous AC molecules of the insect cells are localized in different membrane microcompartments. At this time, we cannot decide whether the second or third explanation is correct or whether both explanations are correct.

Our data on the differential activation of AC by  $\beta_1$ AR-G<sub>s<sub>z</sub></sub> and  $\beta_2$ AR-G<sub>s<sub>z</sub></sub> fusion proteins may help us to understand some of the controversial results regarding AC activation by those GPCRs in non-fused systems. Specifically, several studies have shown that the agonist-occupied  $\beta_1$ AR and  $\beta_2$ AR are similarly efficient at activating AC [7,8,13,14]. These data would be compatible with the assumption that the  $\beta_1$ AR and  $\beta_2$ AR preferentially couple to G<sub>s<sub>S</sub></sub> in those systems (Table 4). However, our data cannot readily explain results showing that the  $\beta_2$ AR is more efficient at activating AC than the  $\beta_1$ AR [9,17] since neither of the two  $\beta_2$ AR-G<sub>s<sub>z</sub></sub> fusion proteins was more efficient at activating AC than the corresponding  $\beta_1$ AR-G<sub>s<sub>z</sub></sub> fusion proteins. It is possible that in a mammalian expression system, the compartmentalization of AC molecules relative to GPCRs and/or G<sub>s<sub>z</sub></sub> differs from the compartmentalization in the insect cell expression system used in this study. Given the fact that the availability of AC molecules limits signal output in  $\beta$ AR/G<sub>s<sub>z</sub></sub> signaling [37,42], it is likely that the localization and/or number of available AC molecules play a major role in determining the efficiencies of  $\beta$ ARs at activating AC in various systems.

In conclusion, coupling of the  $\beta_1$ AR and  $\beta_2$ AR to G<sub>s<sub>z</sub></sub> splice variants is similar in terms of ternary complex formation. G<sub>s<sub>z</sub>L</sub> confers the properties of constitutive activity to the  $\beta_1$ AR and  $\beta_2$ AR, whereas the  $\beta_1$ AR and  $\beta_2$ AR coupled to G<sub>s<sub>S</sub></sub> are not constitutively active.  $\beta_1$ AR-G<sub>s<sub>z</sub>L</sub> and  $\beta_2$ AR-G<sub>s<sub>z</sub>L</sub> differ from each other in their specific efficacies at activating AC. Our data could explain some of the discrepancies in the literature regarding similarities/dissimilarities in ternary complex formation, constitutive activity, and AC activation between the  $\beta_1$ AR and the  $\beta_2$ AR.

## Acknowledgments

We should like to thank the reviewers of this paper for their thoughtful comments. This work was supported by a grant of the Army Research Office (DAAD 19-00-1-0069), the J. R. & Inez Jay Biomedical Research Award of The University of Kansas, and a New Faculty Award of The University of Kansas to R.S.

## References

- [1] Gilman AG. G proteins: transducers of receptor-generated signals. *Annu Rev Biochem* 1987;56:615–49.
- [2] Birnbaumer L, Abramowitz J, Brown AM. Receptor-effector coupling by G proteins. *Biochim Biophys Acta* 1990;1031:163–224.
- [3] Lefkowitz RJ, Cotecchia S, Samama P, Costa T. Constitutive activity of receptors coupled to guanine nucleotide regulatory proteins. *Trends Pharmacol Sci* 1993;14:303–7.
- [4] Gudermann T, Schöneberg T, Schultz G. Functional and structural complexity of signal transduction via G-protein-coupled receptors. *Annu Rev Neurosci* 1997;20:399–427.
- [5] Kobilka BK. Adrenergic receptors as models for G protein-coupled receptors. *Annu Rev Neurosci* 1992;15:87–114.
- [6] Mason DA, Moore JD, Green SA, Liggett SB. A gain-of-function polymorphism in a G-protein coupling domain of the human  $\beta_1$ -adrenergic receptor. *J Biol Chem* 1999;274:12670–4.
- [7] Suzuki T, Nguyen CT, Nantel F, Bonin H, Valiquette M, Frielle T, Bouvier M. Distinct regulation of  $\beta_1$ - and  $\beta_2$ -adrenergic receptors in Chinese hamster fibroblasts. *Mol Pharmacol* 1992;41:542–8.
- [8] Zhou XM, Pak M, Wang Z, Fishman PH. Differences in desensitization between human  $\beta_1$ - and  $\beta_2$ -adrenergic receptors stably expressed in transfected hamster cells. *Cell Signal* 1995;7:207–17.
- [9] Rousseau G, Nantel F, Bouvier M. Distinct receptor domains determine subtype-specific coupling and desensitization phenotypes for human  $\beta_1$ - and  $\beta_2$ -adrenergic receptors. *Mol Pharmacol* 1996;49:752–60.
- [10] Shiina T, Kawasaki A, Nagao T, Kurose H. Interaction with  $\beta$ -arrestin determines the difference in internalization behavior between  $\beta_1$ - and  $\beta_2$ -adrenergic receptors. *J Biol Chem* 2000;275:29082–90.
- [11] Freissmuth M, Selzer E, Marullo S, Schütz W, Strosberg AD. Expression of two human  $\beta$ -adrenergic receptors in *Escherichia coli*: functional interaction with two forms of the stimulatory G protein. *Proc Natl Acad Sci USA* 1991;88:8548–52.
- [12] Green SA, Holt BD, Liggett SB.  $\beta_1$ - and  $\beta_2$ -Adrenergic receptors display subtype-selective coupling to G<sub>s</sub>. *Mol Pharmacol* 1992;41:889–93.
- [13] Green SA, Liggett SB. A proline-rich region of the third intracellular loop imparts phenotypic  $\beta_1$ - versus  $\beta_2$ -adrenergic receptor coupling and sequestration. *J Biol Chem* 1994;269:26215–9.
- [14] Lattion A, Abuin L, Nenniger-Tosato M, Cotecchia S. Constitutively active mutants of the  $\beta_1$ -adrenergic receptor. *FEBS Lett* 1999;457:302–6.
- [15] Zhou YY, Yang D, Zhu WZ, Zhang SJ, Wang DJ, Rohrer DK, Devic E, Kobilka BK, Lakatta EG, Cheng H, Xiao RP. Spontaneous activation of  $\beta_2$ - but not  $\beta_1$ -adrenoceptors expressed in cardiac myocytes from  $\beta_1\beta_2$  double knockout mice. *Mol Pharmacol* 2000;58:887–94.
- [16] Engelhardt S, Grimmer Y, Fan GH, Lohse MJ. Constitutive activity of the human  $\beta_1$ -adrenergic receptor in  $\beta_1$ -receptor transgenic mice. *Mol Pharmacol* 2001;60:712–7.
- [17] Levy FO, Zhu X, Kaumann AJ, Birnbaumer L. Efficacy of  $\beta_1$ -adrenergic receptors is lower than that of  $\beta_2$ -adrenergic receptors. *Proc Natl Acad Sci USA* 1993;90:10798–802.
- [18] Graziano MP, Freissmuth M, Gilman AG. Expression of G<sub>s<sub>z</sub></sub> in *Escherichia coli*. Purification and properties of two forms of the protein. *J Biol Chem* 1989;264:409–18.
- [19] Seifert R, Wenzel-Seifert K, Lee TW, Gether U, Sanders-Bush E, Kobilka BK. Different effects of G<sub>s<sub>z</sub></sub> splice variants on  $\beta_2$ -adrenoceptor-mediated signaling. The  $\beta_2$ -adrenoceptor coupled to the long splice variant of G<sub>s<sub>z</sub></sub> has properties of a constitutively active receptor. *J Biol Chem* 1998;273:5109–16.
- [20] Seifert R. Monovalent anions differentially modulate coupling of the  $\beta_2$ -adrenoceptor to G<sub>s<sub>z</sub></sub> splice variants. *J Pharmacol Exp Ther* 2001;298:840–7.
- [21] Mumby SM, Kahn RA, Manning DR, Gilman AG. Antisera of designed specificity for subunits of guanine nucleotide-binding regulatory proteins. *Proc Natl Acad Sci USA* 1986;83:265–9.
- [22] Wenzel-Seifert K, Seifert R. Molecular analysis of  $\beta_2$ -adrenoceptor coupling to G<sub>s<sub>z</sub></sub>, G<sub>i<sub>z</sub></sub>, and G<sub>q<sub>z</sub></sub>-proteins. *Mol Pharmacol* 2000;58:954–66.
- [23] Bertin B, Freissmuth M, Jockers R, Strosberg AD, Marullo S. Cellular signaling by an agonist-activated receptor/G<sub>s<sub>z</sub></sub> fusion protein. *Proc Natl Acad Sci USA* 1994;91:8827–31.

- [24] Seifert R, Wenzel-Seifert K, Kobilka BK. GPCR-G<sub>α</sub> fusion proteins: an approach for the molecular analysis of receptor/G-protein coupling. *Trends Pharmacol Sci* 1999;20:383–9.
- [25] Milligan G. Insights into ligand pharmacology using receptor-G-protein fusion proteins. *Trends Pharmacol Sci* 2000;21:24–8.
- [26] Wenzel-Seifert K, Arthur JM, Liu HY, Seifert R. Quantitative analysis of formyl peptide receptor coupling to G<sub>i</sub>α<sub>1</sub>, G<sub>i</sub>α<sub>2</sub>, and G<sub>i</sub>α<sub>3</sub>. *J Biol Chem* 1999;274:33259–66.
- [27] Liu H-Y, Wenzel-Seifert K, Seifert R. The olfactory G-protein G<sub>olf</sub> possesses a lower GDP-affinity and deactivates more rapidly than G<sub>Sz</sub><sub>short</sub>: consequences for receptor-coupling and adenylyl cyclase activation. *J Neurochem* 2001;78:325–38.
- [28] Seifert R, Lee TW, Lam VT, Kobilka BK. Reconstitution of β<sub>2</sub>-adrenoceptor-GTP-binding-protein interaction in Sf9 cells: high coupling efficiency in a β<sub>2</sub>-adrenoceptor-G<sub>Sz</sub> fusion protein. *Eur J Biochem* 1998;255:369–82.
- [29] Frielle T, Collins S, Daniel KW, Caron MG, Lefkowitz RJ, Kobilka BK. Cloning of the cDNA for the human β<sub>1</sub>-adrenergic receptor. *Proc Natl Acad Sci USA* 1987;84:7920–4.
- [30] Hoare SRJ. G-protein-coupled receptors: what limits high-affinity agonist binding? *Trends Pharmacol Sci* 2000;21:82–3.
- [31] Seifert R, Wenzel-Seifert K, Kobilka BK. G-protein-coupled receptors: what limits high-affinity agonist binding? Reply. *Trends Pharmacol Sci* 2000;21:83–4.
- [32] Kent RS, De Lean A, Lefkowitz RJ. A quantitative analysis of β-adrenergic receptor interactions: resolution of high and low affinity states of the receptor by computer modeling of ligand binding data. *Mol Pharmacol* 1980;17:14–23.
- [33] Wise A, Sheehan M, Rees S, Lee M, Milligan G. Comparative analysis of the efficacy of A<sub>1</sub> adenosine receptor activation of G<sub>i/o</sub>α G proteins following coexpression of receptor and G protein and pression of A<sub>1</sub> adenosine receptor-G<sub>i/o</sub>α fusion proteins. *Biochemistry* 1999;38: 2272–8.
- [34] Seifert R, Wenzel-Seifert K, Gether U, Kobilka BK. Functional differences between full and partial agonists: Evidence for ligand-specific receptor conformations. *J Pharmacol Exp Ther* 2001;297: 1218–26.
- [35] Seifert R, Gether U, Wenzel-Seifert K, Kobilka BK. The effect of guanine-, inosine- and xanthine nucleotides on β<sub>2</sub>-adrenoceptor/G<sub>s</sub> interactions: evidence for multiple receptor conformations. *Mol Pharmacol* 1999;56:348–58.
- [36] Yagami T. Differential coupling of glucagon and β-adrenergic receptors with the small and large forms of the stimulatory G protein. *Mol Pharmacol* 1995;48:849–54.
- [37] Gao M, Ping P, Post S, Insel PA, Tang R, Hammond HK. Increased expression of adenylylcyclase type VI proportionately increases β-adrenergic receptor-stimulated production of cAMP in neonatal rat cardiac myocytes. *Proc Natl Acad Sci USA* 1998;95: 1038–43.
- [38] Wenzel-Seifert K, Lee TW, Seifert R, Kobilka BK. Restricting mobility of G<sub>s</sub>α relative to the β<sub>2</sub>-adrenoceptor enhances adenylyl cyclase activity by reducing G<sub>s</sub>α GTPase activity. *Biochem J* 1998;334:519–24.
- [39] Matesic DF, Manning DR, Wolfe BB, Luthin GR. Pharmacological and biochemical characterization of complexes of muscarinic acetylcholine receptor and guanine nucleotide-binding protein. *J Biol Chem* 1989;264:21638–45.
- [40] Rebois RV, Warner DR, Basi NS. Does subunit dissociation necessarily accompany the activation of all heterotrimeric G proteins? *Cell Signal* 1997;9:141–51.
- [41] Chidiac P. Rethinking receptor-G protein-effector interactions. *Biochem Pharmacol* 1998;55:549–56.
- [42] Ostrom RS, Post SR, Insel PA. Stoichiometry and compartmentation in G protein-coupled receptor signaling: implications for therapeutic interventions involving G<sub>s</sub>. *J Pharmacol Exp Ther* 2000;294: 407–12.